

## SUB-CELLULAR DISTRIBUTION OF UNC-104(KIF1A) UPON BINDING TO ADAPTORS AS UNC-16(JIP3), DNC-1(DCTN1/Glued) AND SYD-2(LIPRIN- $\alpha$ ) IN *C. ELEGANS* NEURONS

C.-C. HSU,<sup>1</sup> J. D. MONCALEANO<sup>1</sup> AND O. I. WAGNER\*

National Tsing Hua University, Institute of Molecular and Cellular Biology and Department of Life Sciences, 30013 Hsinchu, Taiwan (PR China)

**Abstract**—The accumulation of cargo (tau, amyloid precursor protein, neurofilaments etc.) in neurons is a hallmark of various neurodegenerative diseases while we have only little knowledge how axonal transport is regulated. Kinesin-3 UNC-104(KIF1A) is the major transporter of synaptic vesicles and recent reports suggest that a cargo itself can affect the motor's activity. Inspecting an interactome map, we identify three putative UNC-104 interactors, namely UNC-16(JIP3), DNC-1(DCTN1/Glued) and SYD-2(Liprin- $\alpha$ ), known to be adaptors in essential neuronal protein complexes. We then employed the novel method bimolecular fluorescence complementation (BiFC) assay to visualize motor-adaptor complexes in the nervous system of living *C. elegans*. Interestingly, the binding of UNC-104 to each adaptor protein results in different sub-cellular distributions and has distinctive effects on the motor's motility. Specifically, if UNC-104 bound to UNC-16, the motor is primarily localized in the soma of neurons while bound to DNC-1, the motor is basically found in axonal termini. On the other hand, if UNC-104 is bound to SYD-2 we identify motor populations mostly along axons. Therefore, these three adaptors inherit different functions in steering the motor to specific sub-cellular locations in the neuron. © 2011 IBRO. Published by Elsevier Ltd. All rights reserved.

**Key words:** bimolecular fluorescence complementation assay (BiFC), axonal transport, JNK-interacting proteins, kinesin-3, dynein, molecular motors.

Axonal transport is increasingly becoming a spotlight in neurodegenerative disorder research. Proper regulation of cargo transport in lengthy, thin and crowded neuronal extensions is critical while malfunction in molecular-motor based transport might lead to accumulation of proteins (e.g. tau, amyloid precursor protein, neurofilaments) in axons, a hallmark of various neurodegenerative diseases. How molecular motors are regulated and how motors recognize their cargo remains largely unknown, however, increasing evidence suggest that cargo-binding is highly specific and that the same motor can bind various types of

cargo. For example, KIF5, a member of the kinesin-1 family, binds amyloid precursor protein (APP) or Apolipoprotein E receptor 2 (ApoER2) containing vesicle through JIPs, on the other hand  $\alpha$ -amino-3-hydroxy-5-methyl-4-isoxazolepropionic acid receptor (AMPA-receptor) containing vesicles are bound via the scaffolding protein glutamate receptor interacting protein 1 (GRIP1). Interestingly, if KIF5 bound to GRIP1, vesicles are steered to dendrites while if bound to JIPs vesicles are directed towards axons (Kaether et al., 2000; Kamal et al., 2000; Verhey et al., 2001; Setou et al., 2002; Inomata et al., 2003; Matsuda et al., 2003). In *C. elegans*, if the conventional kinesin-1 heavy chain homolog UNC-116 binds the JNK-interacting protein UNC-16, vesicles are specifically directed to axons while avoiding dendrites (Byrd et al., 2001). Another example is that upon binding of the active zone protein SYD-2(Liprin- $\alpha$ ) to kinesin-3 UNC-104(KIF1A), the motor's anterograde destinations are favored limiting movements backwards to the soma (Wagner et al., 2009). These examples demonstrate that direct and specific binding of cargo to a motor determines the destination (axons vs. dendrites) and/or directionality (anterograde vs. retrograde) of a motor or vesicular cargo (for review; Hirokawa et al., 2009b).

To gain more insight about the specificity of motor-cargo binding and how a cargo (precursor proteins, vesicular structures, adaptors etc.) regulate the destination of a motor, we used an interactome map (Zhong and Sternberg, 2006) to identify putative binding partners for the major synaptic vesicle transporter UNC-104(KIF1A) in *C. elegans*. We identified three proteins UNC-16(JIP3), DNC-1(DCTN1/Glued) and SYD-2(Liprin- $\alpha$ ), while all of them have in common to be engaged as adaptors in essential neuronal protein complexes. For example, UNC-16 is known to act as a scaffold protein, binding to the light chain of kinesin-1 (KLC-2) and regulating the transport of synaptic vesicle components by combining kinesin-1 transport and JNK signaling (Byrd et al., 2001; Sakamoto et al., 2005; Brown et al., 2009). It has also been hypothesized that UNC-16 might trigger directionality of cargo by mediating the interaction between kinesin-1 and dynein through its association with p150<sup>Glued</sup> (Sakamoto et al., 2005; Koushika, 2008; Montagnac et al., 2009). JIP3 facilitates JNK phosphorylation of APP and JIP3 gene disruption in mice leads to defects in axon guidance that may be due to reduced vesicle transport, as observed in *unc-16* mutants in *C. elegans* (Kelkar et al., 2003). There is no study, however, on direct interactions between UNC-16 and UNC-104 and the effect on the motor's neuronal distribu-

<sup>1</sup> These authors contributed equally to this work.

\*Corresponding author. Tel: +886-3-574-2487; fax: +886-3-571-5934.

E-mail address: owagner@life.nthu.edu.tw (O. I. Wagner).

**Abbreviation:** BiFC assay, bimolecular fluorescence complementation assay; JIP, JNK-interacting protein; JIP3, JNK-interacting protein 3 (or also termed JNK/stress-activated protein kinase-associated protein 1, JSAP1); JNK, c-Jun N-terminal kinase; LAR, leucocyte common antigen-related protein receptor; Liprin, LAR-interacting protein.

tion. The second identified UNC-104 interactor, DNC-1 (DCTN1/Glued), is a homolog of p150<sup>Glued</sup>, a component of the dynactin complex which is an important adaptor to connect the retrograde motor dynein to both the cargo (vesicle) and the microtubule. It has been suggested that bidirectional movement of synaptic vesicles is a result of opposing molecular motors (bound to one vesicle at the same time) pulling in different directions in a tug-of-war event or as a result of coordinated activity (for review; Holzbaur and Goldman, 2010). Indeed, direct interactions between kinesin-II and p150<sup>Glued</sup> (Deacon et al., 2003), kinesin-I and dynein (Ligon et al., 2004) and indirect interactions between UNC-104 (Koushika et al., 2004) as well as a *Drosophila* UNC-104 homolog (Barkus et al., 2008) and dynein have been reported. However, direct interactions between UNC-104 and dynactin (or dynein) and the resulting sub-cellular distribution of the motor remains to be unsolved. The third UNC-104 interactor, SYD-2/Liprin- $\alpha$ , is a key player in assembling and regulating active zones (electron dense regions at the synapse at which synaptic vesicle fusion and transmitter release occurs). Through its multifunctional interaction with Rab3-interacting molecule (RIM), LAR and calcium/calmodulin-dependent serine protein kinase 3 (CASK) it mediates targeting the presynaptic transmission machinery to opposite postsynaptic densities (Olsen et al., 2006). Interactions between UNC-104 and SYD-2/Liprin- $\alpha$  have been reported (Wagner et al., 2009), however, it remains unclear how the motor's sub-cellular distribution changes upon direct binding to SYD-2.

UNC-104, a homologue of the mammalian kinesin-3 KIF1A, is a neuron-specific, microtubule plus-end directed motor and is the major transporter of synaptic vesicles in axons. Mutations in the UNC-104 gene in worms result in uncoordinated, slow body motion and a slow growth rate while the concentration of synaptic vesicles increases in cell bodies and decreases at synapses (Hall and Hedgecock, 1991). KIF1A knockout mice are lethal with motor and sensory defects and abnormal distribution of synaptic vesicles (retained in soma and reduced in neuronal terminals) (Yonekawa et al., 1998). In *C. elegans*, fluorescently labeled UNC-104 reveals a bidirectional moving pattern with net transport rates in anterograde directions (Zhou et al., 2001; Wagner et al., 2009).

We use a novel method, bimolecular fluorescence complementation (BiFC) assay, to visualize protein–protein interaction in living animals. The method is based on the principle of protein-fragment complementation using two non-fluorescent fragments derived from fluorescent proteins. When two hybrids of fluorescent proteins are brought together in living cells (by fusing each to one of a pair of interacting proteins) fluorescence is restored (Hu and Kerppola, 2003; Kerppola, 2006a,b; Shyu et al., 2008; Zal, 2008). This not only enables to identify direct and physical interactions between two proteins but also their sub-cellular localization upon interaction.

## EXPERIMENTAL PROCEDURES

### C. *elegans* strains and plasmids

*C. elegans* strains were maintained at 22 °C using standard methods (Brenner, 1974). For BiFC assays, we used the BiFC control vector kit (pCE::bJUN::VN173 and pCE::bFOS::VC155) from Dr. Chang-Deng Hu's Laboratory (Purdue University, USA) and replaced the heat shock promoter hsp16.41 with the pan-neuronal Punc-104 promoter. Positive control vectors for nucleus expression Punc-104::bJUN::VN173 (40  $\mu$ g/ml) and Punc-104::bFOS::VC155 (30  $\mu$ g/ml), respectively, were microinjected into N2 hermaphrodites using the pRF4 rol-6(su1006) co-injection marker (employing standard microinjection methods; Mello et al., 1991). Positive control vectors for investigating neuronal expression of two known interacting proteins (UNC-104/UNC-104), Punc-104::UNC-104::VN173 (60  $\mu$ g/ml) and Punc-104::UNC-104::VC155 (60  $\mu$ g/ml), were microinjected into CB1265 unc-104(e1265) hermaphrodites rescuing the highly uncoordinated and paralytic phenotype (note, that the need of high plasmid dosages to rescue the *unc-104* phenotype has been reported previously; Wagner et al., 2009). To determine (reported) UNC-16/KLC-2 interactions (used as a positive control) we made a worm expressing Punc-104::UNC-16::VN173/Punc-104::KLC-2::VC155 BiFC pairs by microinjecting a Punc-104::UNC-16::VN173 (50  $\mu$ g/ml) plasmid and a Punc-104::KLC-2::VC155 (50  $\mu$ g/ml) plasmid into N2 strains (using the co-injection marker pRF4). As a negative control, we deleted UNC-16's KLC-2 binding domain and injected a Punc-104::UNC-16 $\Delta$ KLCBD::VN173 (50  $\mu$ g/ml) plasmid and a Punc-104::KLC-2::VC155 (50  $\mu$ g/ml) plasmid into N2 strains (using the co-injection marker pRF4). To determine reported UNC-16/DNC-1 interactions (also used as a positive control) we designed a worm expressing Punc-104::UNC-16::VN173/Punc-104::DNC-1::VC155 BiFC pairs by microinjecting a Punc-104::UNC-16::VN173 (60  $\mu$ g/ml) plasmid and a Punc-104::DNC-1::VC155 (60  $\mu$ g/ml) plasmid into N2 strains (with co-injection marker pRF4).

To evaluate UNC-16/UNC-104 expression, we designed a worm expressing Punc-104::UNC-16::VN173/Punc-104::UNC-104::VC155 BiFC pairs by microinjecting a Punc-104::UNC-16::VN173 (50  $\mu$ g/ml) and a Punc-104::UNC-104::VC155 (50  $\mu$ g/ml) plasmid into the strain CB1265 unc-104(e1265) rescuing the *unc-104* phenotype. To investigate UNC-104/DNC-1 interactions a strain expressing Punc-104::UNC-104::VN173/Punc-104::DNC-1::VC155 BiFC pairs was generated by microinjecting a Punc-104::UNC-104::VN173 (50  $\mu$ g/ml) plasmid and a Punc-104::DNC-1::VC155 (50  $\mu$ g/ml) plasmid into the CB1265 unc-104(e1265) line rescuing the *unc-104* phenotype. For SYD-2/UNC-104 interactions, we designed worms expressing a Punc-104::VN173::SYD-2/Punc-104::UNC-104::VC155 BiFC pair by microinjecting a Punc-104::VN173::SYD-2 plasmid (60  $\mu$ g/ml) and Punc-104::UNC-104::VC155 plasmid (70  $\mu$ g/ml) into the CB1265 unc-104(e1265) strain rescuing the highly uncoordinated phenotype. Strains expressing Punc-104::UNC-104::GFP (to evaluate UNC-104 expression alone) have been described elsewhere (Wagner et al., 2009).

### Primary neuronal cell culture

Primary neuronal cells from *C. elegans* were isolated according to the protocols by Christensen et al. (2002) and Strange et al. (2007). In brief, primary neuronal cells are isolated from embryonic eggs collected from L4 worms. To free eggs from a worm, the epidermis of the worm is lysed (in a solution containing high molar NaOH and bleach (NaClO)) whereas the eggs—containing a resistant chorion (chitin-shell)—are not negatively affected by the lysis process. After separating the eggs from the worm debris using sucrose centrifugation, the eggs are subsequently treated with the enzyme chitinase to digest the egg shell. The released embryonic cells are then

dissociated (by repeatedly pipetting) and plated on glass-bottomed dishes (MatTek, USA) coated with peanut lectin (Sigma, USA). Nematode cells can be stored at 22 °C and do not need CO<sub>2</sub>.

### Whole worm microscopy, motor motility analysis and quantification of fluorescence in cells

For imaging of BiFC pair expression in living animals, worms were immobilized by treatment with 5 mM levamisole (Sigma, USA) before being placed on 2% agarose-coated objective slides. We either used an Olympus FV1000 (for morphological studies) or an Olympus IX81 microscope with a DSU Nipkow spinning disk unit connected to an Andor iXon DV887 EMCCD camera for time-lapse imaging at 1–2 frames per s (motor motility analysis). To convert recorded time-lapse sequences into kymographs, we used the image analysis software NIH ImageJ 1.43. In detail, a line over the axon of interest is drawn, followed by the application of the “reslice stack function.” Static particles appear as vertical lines whereas the slope of moving particles corresponds to the velocity of the particle. A pause is defined if motors move less than 0.085 μm/s while each calculated velocity does not contain any pausing event. Examples of what is regarded as a single moving event (slope) are given in Fig. 7B. Vertical lines from static particles were used to correct for mechanical drifts of the microscope stage. Curved objects (for example isolated neuronal cells) were straightened before their conversion into kymographs using the “straighten curved objects tool” from Kocsis et al. (1991). Run length is defined as “net moving distance” (or processivity) and is calculated from the start to the end of the respective recording time (including all pauses and motor reversals). Moving persistency is defined as the time of constant movements without pausing, stop and starts. Data from different experimental groups were compared using the Student *t*-test (two tailed and unequal variance).

For quantification of cellular fluorescence pattern (with gray values as arbitrary units of fluorescence), we first straightened curved axons and then applied line scans using ImageJ’s “plot profile” function. For quantification of fluorescence in soma and axonal termini we determined percentages of the areas under the curves (positive integrals) obtained from line scans. Wavelength scans along whole worms (to detect Venus fluorescence in negative control experiments) were performed by employing the wavelength scan function of an Olympus FV1000 confocal laser scanning microscope.

## RESULTS

### Comparison of UNC-104::GFP and UNC-104::VN/UNC-104::VC expression

We use a novel technique BiFC assay to investigate the sub-cellular distribution of the molecular motor UNC-104 in the nervous system of living *C. elegans* and in cultures of primary *C. elegans* neurons. Fig. 1A summarizes the basic principles of the BiFC assay: two proteins (A and B) are fused to either a (non-fluorescent) N-terminal (VN173) or a C-terminal (VC155) fragment of a (yellow fluorescent) Venus protein. If direct interaction occurs between two proteins, Venus hybrids are close enough to complement and fluorescence is restored. A long linker composed of 15 amino acids (for details; Shyu et al., 2008) connects the proteins (to be assayed) with the respective Venus hybrid allowing them to retain their inherent dynamics (for example upon interacting with other proteins). To understand how the motor UNC-104 is expressed in worms and cells, we evaluated the expression pattern of an existing worm expressing UNC-104::GFP alone (Wagner et al., 2009). Fig. 1 shows the pan-neuronal

expression of UNC-104 in the head (Fig. 1B), including the nerve ring and sensory neurons, in the dorsal and ventral nerve cord (Fig. 1C, D), as well as in the tail (Fig. 1E). Isolated cells reveal uniform expression of the motor from the soma to the tip (termini) (Fig. 1F, G).

We then employed a well documented positive control for BiFC assay (the interaction between bJUN and bFOS in nuclei; Hu et al., 2002; Hiatt et al., 2008); however, using a Punc-104 promoter for restriction to neuronal tissue expression. Indeed nucleus expression of the bZIP domains of transcription factors FOS-1 and JUN-1 was obvious in the nerve ring of *C. elegans* (Fig. 2A). Note that injection of empty vectors (only containing the gateway cassette) Punc-104::GW::VN173 and Punc-104::GW::VC155 did not lead to any detectable Venus expression. Another positive control was employed by testing for UNC-104/UNC-104 interactions. As it is well known that (non-processive) UNC-104 monomers interact to form dimers (enabling the motor to move processively along microtubules) (for review; Hirokawa et al., 2009a) we expressed a BiFC pair composed of an UNC-104::VN173 and an UNC-104::VC155 construct. The expression was obvious throughout the nervous system including sensory neurons in the head (Fig. 2B) and dorsal and ventral nerve cords (Fig. 2D). Also in isolated *C. elegans* neurons (Fig. 2C) expression is comparable to UNC-104::GFP expression (Fig. 1F). To understand if unspecific VN/VC self-interactions exist, we performed line-scans along UNC-104::GFP and UNC-104::VN/UNC-104::VC expressing neurons. Inspecting regions of least expression in Fig. 2E (for example at the section between 8 μm and 24 μm) it is obvious that no significant differences exist between UNC-104::GFP and UNC-104::VN/UNC-104::VC expression, therefore pointing to negligible VN/VC self-interactions. Further, the overall expression pattern of UNC-104::GFP compared to UNC-104::VN/UNC-104::VC is comparable with typical UNC-104 clustering along axons (Wagner et al., 2009) and in between only little (if not any) axoplasmic expression.

### UNC-104 distribution upon binding to UNC-16

Expressing UNC-104::VC155 and UNC-16::VN173 at the same time in living *C. elegans* allows for the observation of specific locations of those UNC-104 motors bound to the adaptor protein UNC-16. Venus complementation (and therefore physical interactions between the motor and adaptor) was evident in the nerve ring (Fig. 3A, D), dorsal/ventral cords and sublateral neurons (Fig. 3B, E) as well as in tail ganglia (Fig. 3C, F). To better understand the sub-cellular distribution of motors when bound to UNC-16, we isolated and cultured primary neurons from these animals. Fig. 3G–J shows the typical distribution of these complexes with 76% expression in the soma, 13% expression along axons and 11% expression in axonal tips (termini) (Fig. 3K). As a positive control, we investigated the documented JIP3(UNC-16)/KLC(KLC-2) interaction (Byrd et al., 2001; Sakamoto et al., 2005) (Fig. 4A) by expressing UNC-16::VN173 and KLC-2::VC155 BiFC pairs in worms (Fig. 4B–D). Interestingly, quantification of the expression pattern reveals a similar distribution of

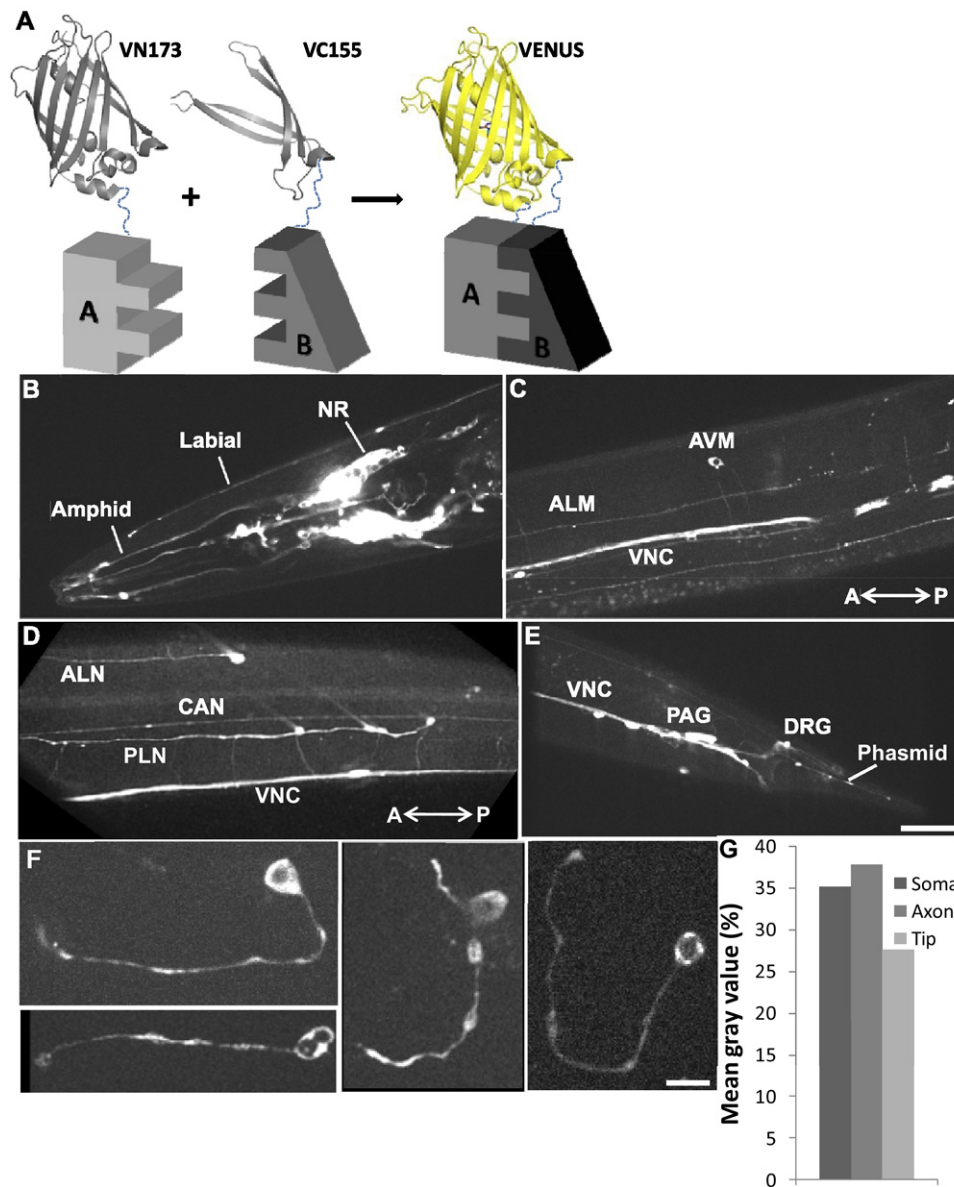


**Fig. 1.** Model of BiFC assay and UNC-104::GFP expression in *C. elegans*. (A) Two proteins (A and B) are fused to Venus hybrids. The split position of the N-terminal Venus hybrid is amino acid 172–173 (VN173) and that of the C-terminal half is 154–155 (VC155). When both proteins (A and B) are close enough for physical interaction, Venus hybrids might complement to form a yellow fluorescent protein. Note that Venus hybrids and fused proteins are connected via a long linker (15 amino acids) so that dynamical movement of fusions is possible. (B–E) Selected areas of *C. elegans* expressing UNC-104::GFP. The protein is solely expressed in nervous tissues. (B) Head of the worm revealing expression in the nerve ring (NR), as well as in sensory neurons (e.g. amphid and labial sensilla). (C, D) UNC-104 expression in nerve cords (VNC), the sublaterals system (e.g. ALN and PLN) as well as mechanosensory neurons (e.g. AVM and ALM). (E) Tail of the worm revealing expression in tail ganglia (e.g. pre-anal and dorso-rectal ganglion) and sensory neurons (phasmid sensilla). (F) Isolated primary neurons from worms expressing UNC-104::GFP revealing a uniform UNC-104 expression (quantified in (G)). Scale bars: 25  $\mu$ m (B–E) and 5  $\mu$ m (F). For interpretation of the references to color in this figure legend, the reader is referred to the Web version of this article.

UNC-16/KLC-2 BiFC (76% soma, 22% axon and 2% tips, Fig. 4H) if compared to UNC-104/UNC-16 (76% soma, 13% axon and 10% tips, Fig. 3K) pointing to a universal role of UNC-16 in similarly regulating the allocation of different types of kinesins. That UNC-16/KLC-2 and UNC-104/UNC-16 are expressed mainly in soma might lead to assumption that unwanted overexpression effects play a role in these types of distributions. Therefore, we investigated another documented interaction,

the binding of UNC-16(JIP3) to DNC-1(p150<sup>Glued</sup>) (Montagnac et al., 2009) (Fig. 4A). Interestingly, when UNC-16 interacts with DNC-1 in *C. elegans* neurons, much higher expression can be seen in axons and tips (46% soma, 23% axons and 32% tips, Fig. 4E–G, I) compared to UNC-16/KLC-2 (Fig. 4H) and UNC-104/UNC-16 (Fig. 3K). As a negative control, we expressed an UNC-16 construct lacking its KLC-2 binding domain (UNC-16 $\Delta$ KLCBD::VN, Fig. 4A, J) together with an

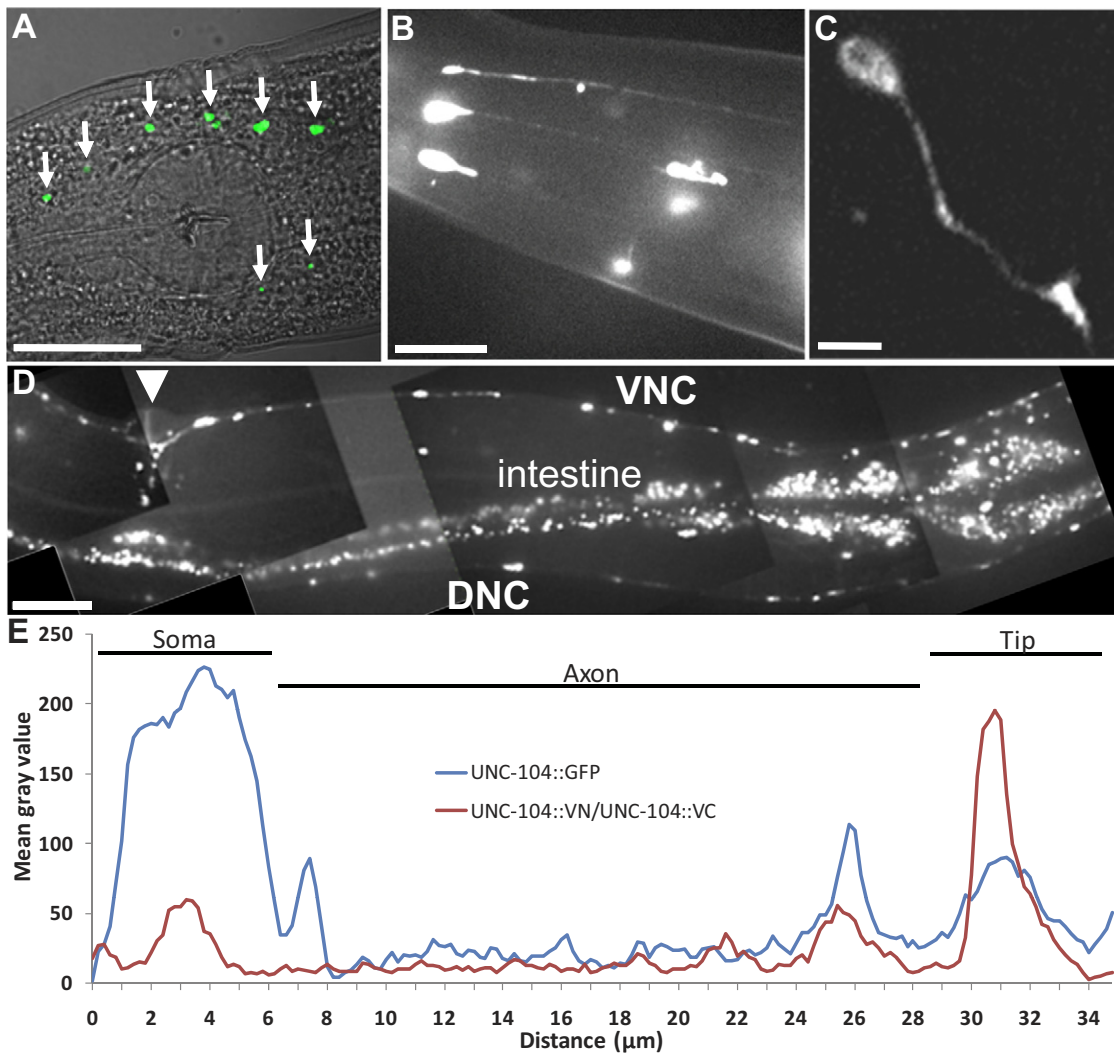


**Fig. 2.** Positive controls and test for VN/VC self-interactions. (A) Yellow fluorescence (here shown by green false color) reveals successful Venus complementation after bJUN/bFOS interactions in nuclei (arrows) of nerve ring neurons. (B) Venus signals after UNC-104/UNC-104 interactions (likely based on motor dimerization events) in head (sensory) neurons of a worm, (C) a single isolated neuron and (D) in dorsal and ventral nerve cords of a worm (arrow head pointing to the vulva). Note the autofluorescence of bacteria (serving as nutriment) in the intestines of the worm partially overlapping with GFP signals (D). (E) Line scan along a neuron expressing UNC-104::GFP compared to a neuron expressing a UNC-104::VN/UNC-104::VC BiFC pair. Comparing areas of least expression (e.g., in a region between 8 and 24  $\mu\text{m}$ ) reveals no obvious differences between UNC-104::GFP and UNC-104::VN/UNC-104::VC assuming that VN/VC self-interactions are low (if not insignificant). Scale bars: 25  $\mu\text{m}$  (A, B and D) and 5  $\mu\text{m}$  (C). For interpretation of the references to color in this figure legend, the reader is referred to the Web version of this article.

KLC-2::VC construct and a *rol-6* marker. As a result, worms revealed the roller phenotype (pointing to successful microinjection of UNC-16 $\Delta$ ::NV/KLC-2::VC BiFC pair) but did not show any significant Venus expression employing whole worm wavelength scans (Fig. 4L).

#### UNC-104 distribution upon binding to DNC-1 and SYD-2

Similar to UNC-104/UNC-16 BiFC pairs, expression of UNC-104/DNC-1 pairs is obvious not only in the nerve ring but also in sensory neurons (Fig. 5A, D) as well as in the dorsal/ventral nerve cords (Fig. 5B, E) and tail ganglia (Fig. 5C, F). However, a closer look at the expression pattern in isolated neurons from these animals reveals a dissimilar motor distribution

if compared to UNC-104/DNC16 complexes: most motors are located in tips (71%) with few expression along axons (19%) and little expression in soma (11%) (Fig. 5G–K).

While direct interactions between UNC-104 and UNC-16 as well as UNC-104 and DNC-1 have not been studied yet, functional interactions between UNC-104 and SYD-2 are well documented (Wagner et al., 2009). However, specific allocations of UNC-104/SYD-2 complexes were not shown in the aforementioned study. Similar to BiFC pairs shown in Figs. 3 and 5, the expression of UNC-104/SYD-2 complexes can be seen in the nerve ring (Fig. 6A, D) as well as in nerve cords (Fig. 6B, C, E, F). Investigating the sub-cellular distribution of motor-adaptor complexes in isolated neurons, only little expression can

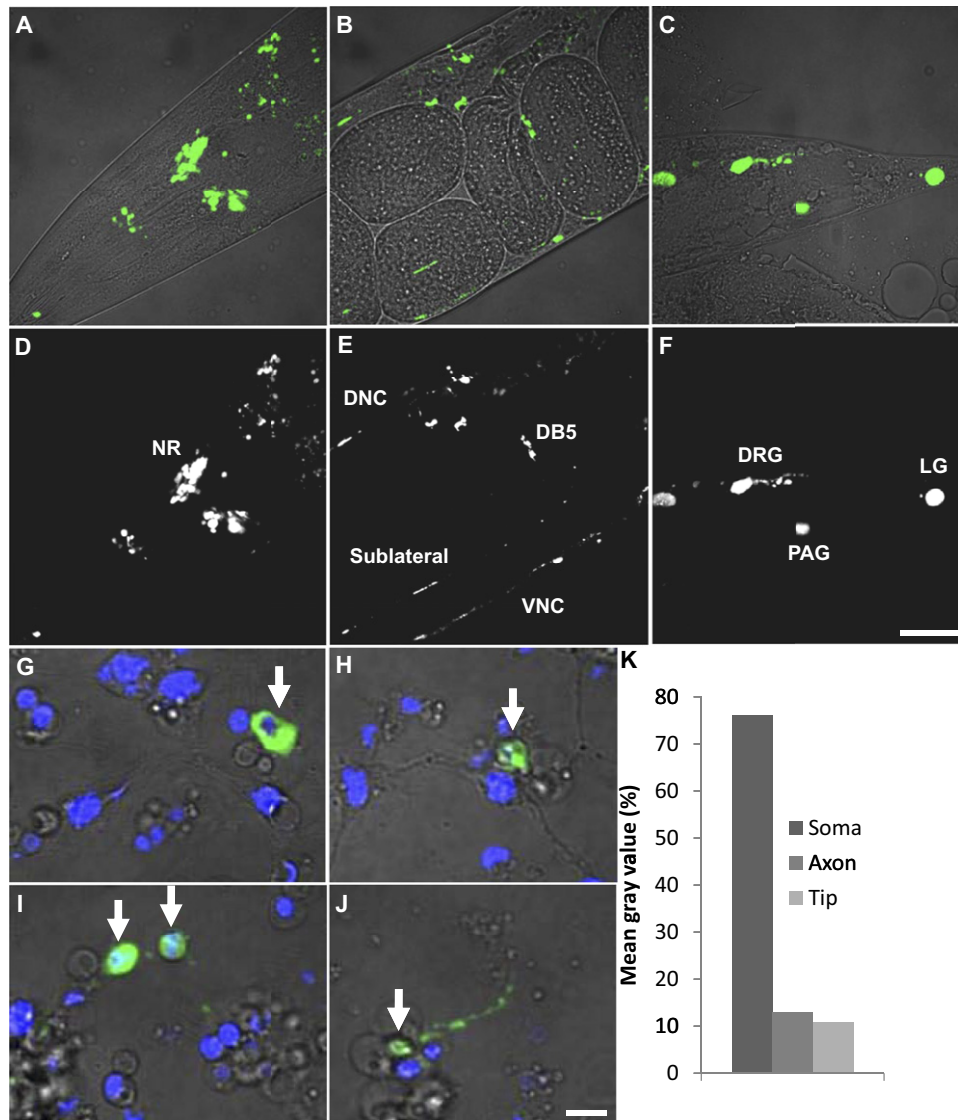


**Fig. 3.** Sub-cellular UNC-104 distribution upon interaction with UNC-16. (A–F) Venus fluorescence was evident in the nervous tissue of *C. elegans* after microinjecting a UNC-104/UNC-16 BiFC pair. (A, D) Head of the worm with expression in the nerve ring (NR). (B, E) Expression in body neurons (dorsal/ventral nerve cord) as well as in the sublateral system. (C, F) Expression in tail ganglia (e.g. dorso-rectal, pre-anal and lumbar ganglion). (G–J) Isolated primary neurons from worms expressing UNC-104/UNC-16 BiFC pairs revealing that UNC-104 (bound to UNC-16) is retained in the soma with little expression in axons and tips (termini) (J) (arrows pointing to cells bodies). Note that (a), expression was not evident in all neurons (nuclei stained with DAPI) and (b), according to Strange et al. (2007), in primary neuronal cultures only about 70% of all cells are neurons (including glial cells) and about 30% muscles cells. (K) Quantification of BiFC expression in isolated neurons (161 cells were analyzed). Scale bars: 25  $\mu\text{m}$  (A–F) and 5  $\mu\text{m}$  (G–J). For interpretation of the references to color in this figure legend, the reader is referred to the Web version of this article.

be seen in soma (9%) with predominant expression in distal parts of axons (64%) but also in growth cones (27%) (Fig. 6G–K). These results suggest that all three adaptors (UNC-16, DNC-1 and SYD-2) inherit different regulatory roles in steering the motor to (or retaining the motor from) different cellular locations.

### Motility pattern of migrating UNC-104/DNC-1 and UNC-104/SYD-2 complexes

We wish to understand whether or not UNC-104's motility changes upon binding to different adaptors. Therefore we set out to record motility pattern of migrating

(J) Comparison of the plasmid size of the full length UNC-16::VN construct and the plasmid with the shorter UNC-16 $\Delta$ KLCBD::VN insert. The UNC-16 $\Delta$ KLCBD::VN/KLC-2::VC BiFC pair was injected into worms together with an *rol-6* co-injection marker to monitor successful generation of transgenic animals. Though worms revealed the typical roller phenotype (pointing to successful microinjection of the UNC-16 $\Delta$ KLCBD::VN/KLC-2::VC BiFC pair (K)), wavelength scans along these worms did not reveal significant Venus signals compared to worms expressing (full-length) UNC-16::VN/KLC-2::VC constructs (L). Thick arrows pointing to cell bodies, thin arrows to axonal expression and arrow heads to tips of axons. Scale bars: 5  $\mu\text{m}$  (B–G) and 500  $\mu\text{m}$  (K). For interpretation of the references to color in this figure legend, the reader is referred to the Web version of this article.

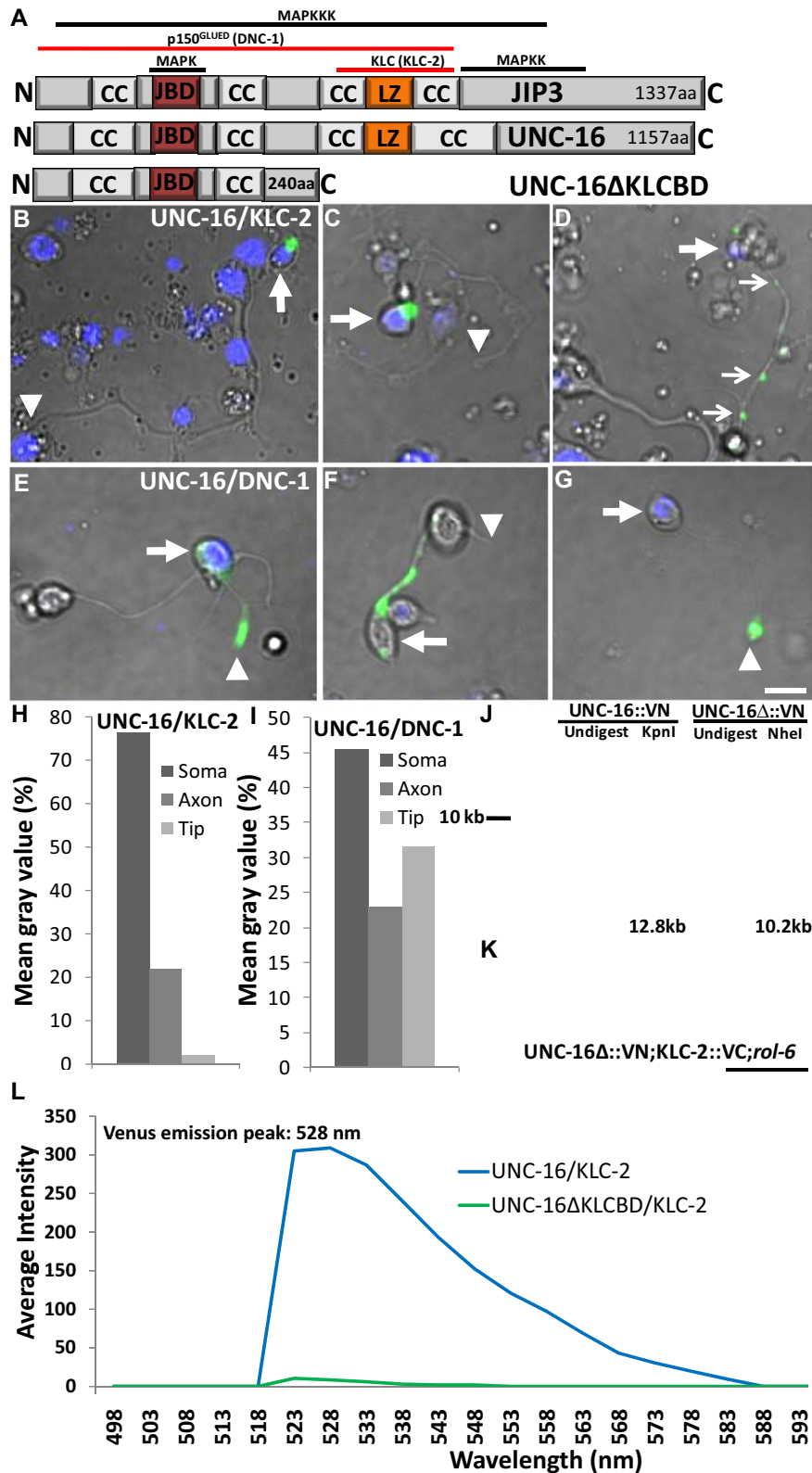


**Fig. 4.** Positive and negative controls for UNC-16 related experiments. (A) Schematic drawing of mammalian JIP3 compared to UNC-16 with marked binding sites of p150<sup>GluED</sup> (DNC-1) and KLC (KLC-2). An UNC-16 construct truncated by its KLC-2 binding domain (UNC-16ΔKLCBD) was used as a negative control (J, K). (B–D) Isolated neurons from worms expressing a KLC-2/UNC-16 BiFC pair (reported interaction used as a positive control). (H) Quantification of expression pattern in cells shown in (B–D) (92 cells were analyzed). (E–G) Isolated neurons from worms expressing a DNC-1/UNC-16 BiFC pair (also used as positive controls based on reported interactions). (I) Quantification of expression pattern in cells shown in (E–G) (21 cells were analyzed).

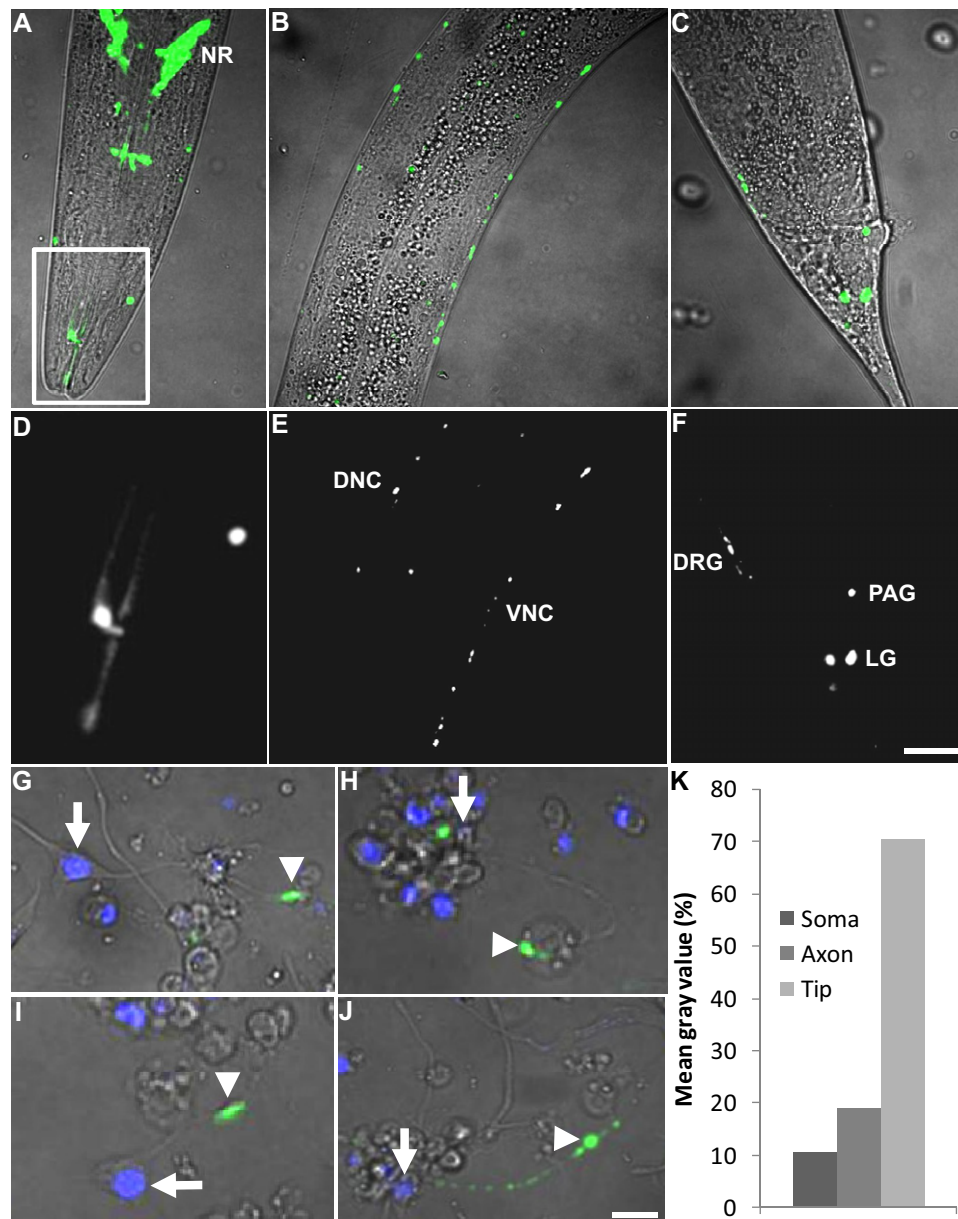


**Fig. 5.** Distribution pattern of UNC-104 while interacting with DNC-1. (A–F) Detection of Venus fluorescence in the nervous system of living worms after expressing a UNC-104/DNC-1 BiFC pair. (A) Fluorescence in the nerve ring and sensory neurons (inset with magnification in (D)). (B, E) Venus signals in dorsal and ventral nerve cords. (C, F) Visible BiFC pairs in tail ganglia. (G–J) Isolated neurons reveal expression primarily in tips of axons and seldom expression all along axons (J) (arrows pointing to cell bodies and arrow heads to tips of axons). (K) Quantification of BiFC expression in neuronal cultures (212 cells were analyzed). Scale bars: 25  $\mu$ m (A–F) and 5  $\mu$ m (G–J). For interpretation of the references to color in this figure legend, the reader is referred to the Web version of this article.

UNC-104::GFP particles alone and compared to UNC-104 in a BiFC complex. As most of UNC-104/UNC-16 complexes retained in soma (Fig. 3) we were not able to record enough data for a statistical useful analysis. However, we could record enough moving events for UNC-104/DNC-1 (Fig. 7) and UNC-104/SYD-2 (Fig. 8) complexes. It is obvious that retrograde moving events of UNC-104/DNC-1 complexes are reduced when compared to UNC-104 motility alone (Fig. 7A) which is consistent with the finding that UNC-104/DNC-1 complexes are retained in growth cones (Fig. 5K). Also overall

speeds and net transport rates are reduced (Fig. 7C, G) while, interestingly, the persistency of movements increased when UNC-104 interacts with DNC-1 (Fig. 7I). As we recorded only few retrograde moving events, we could only provide statistical useful data for anterograde movements in Fig. 7.

Compared to UNC-104::GFP movements alone, UNC-104/SYD-2 particles showed reduced velocities, processivity (net transport) and moving persistency in both, anterograde and retrograde directions (Fig. 8A–F) whereas the percentage of retrograde movements are

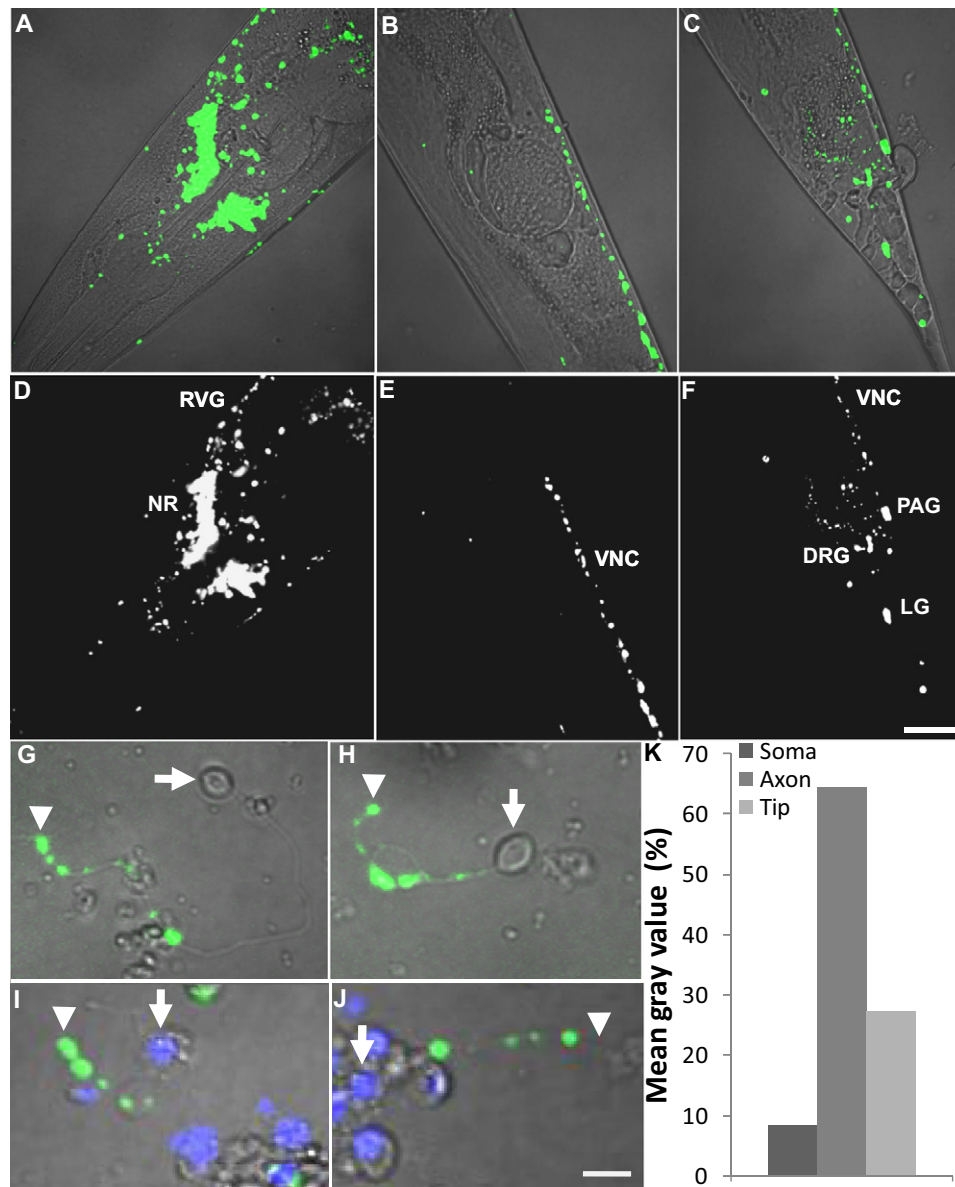


**Fig. 6.** Expression of UNC-104/SYD-2 BiFC pairs in *C. elegans*. (A–F) Venus complementation in the nervous system of living worms upon physical interactions between VN173::SYD-2 and UNC-104::VC155. (A, D) Expression of the UNC-104/SYD-2 BiFC pair is evident in the nerve ring (including the retrovesicular ganglion) as well as in nerve cords (B, E) and tail ganglia (C, F). Note that expression was limited to only a subset of neurons. (G–J) Expression of BiFC pairs in isolated neurons reveals expression mostly in distal parts of the axons but also in tips (arrow pointing to cell bodies and arrow heads to tips). Images in (G + H) taken from an independent experiment without DAPI staining. (K) Quantification of Venus expression in isolated neurons (80 cells were analyzed). Scale bars: 25  $\mu$ m (A–F) and 5  $\mu$ m (G–J). For interpretation of the references to color in this figure legend, the reader is referred to the Web version of this article.

slightly increased (Fig. 8G) (see Discussion for details).

## DISCUSSION

Based on lengthy, thin and crowded neuronal processes it is not surprising that failure of cargo transport might lead to accumulation of disease proteins. Therefore, the role of axonal transport on neurodegenerative diseases is broadly discussed in the literature (Chevalier-Larsen and Holzbaur, 2006; Duncan and Goldstein, 2006; Stokin and Goldstein, 2006; De Vos et al., 2008; Morfini et al., 2009). On

the other hand, only little is known how molecular motors are regulated in the nervous system and only in recent years evidence appears that roughly five major factors involve in the regulation. First, post-translational modification of microtubules have a significant effect on motor distribution and activity; second, the cargo itself is able to activate, deactivate and even control the directionality of motors; third, intramolecular folding of motors play a role in motor regulation, while the folding itself can be released upon cargo-binding; fourth, bidirectional movement of vesicles and cargo might be based on tug-of-war mechanism

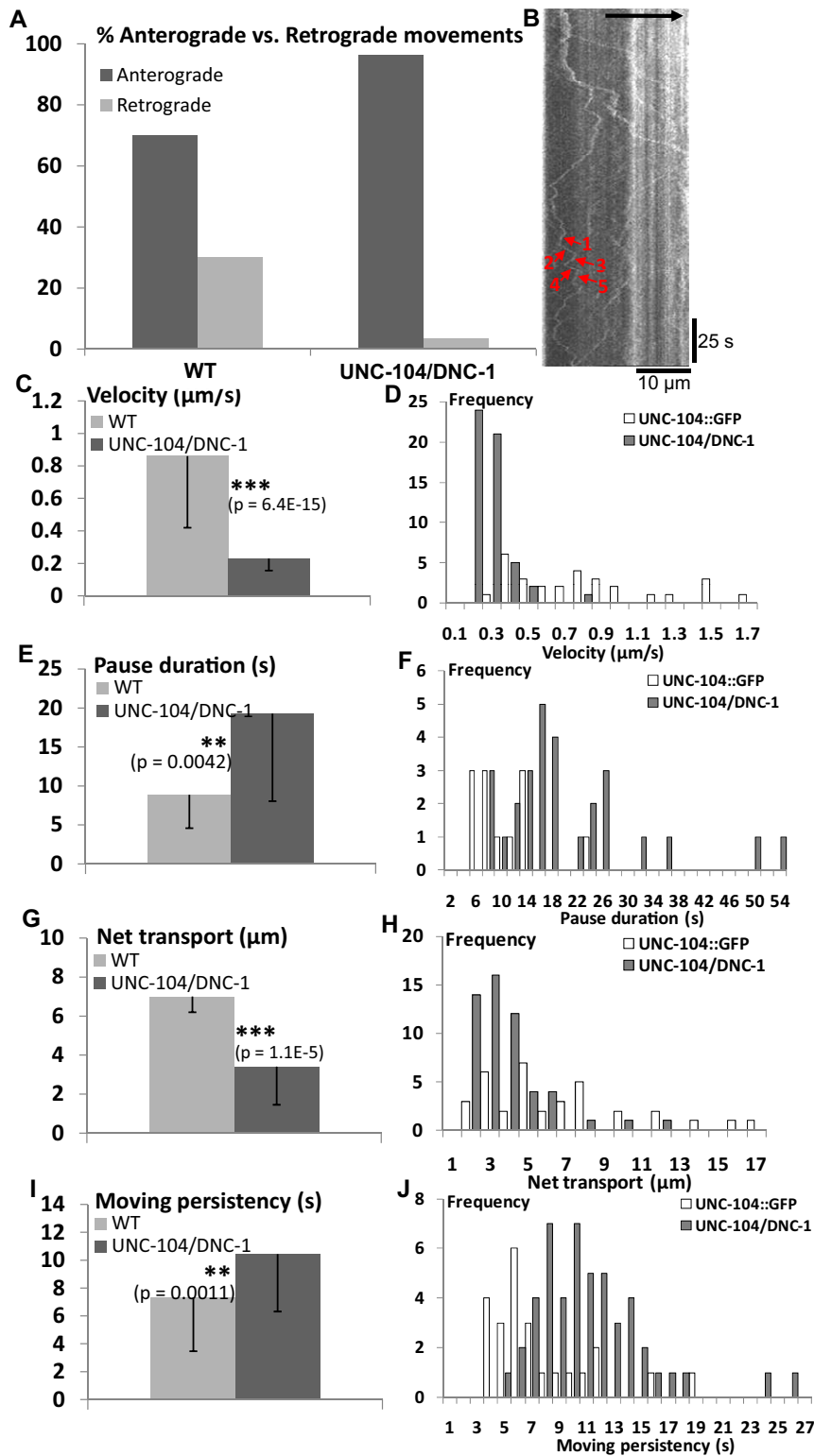


**Fig. 7.** Motility analysis of UNC-104/DNC-1 movements compared to UNC-104 alone. (A) Analysis of the percentage of anterograde movements versus retrograde movements of UNC-104::GFP alone (WT) or UNC-104 bound to DNC-1. (B) Example of a kymograph for UNC-104::GFP motility. Black arrows pointing to examples what we regard a "single event" used for motility analysis (a pause was defined as a velocity of less than  $0.085 \mu\text{m/s}$ ). Red arrows pointing to examples what we regard a "single event" used for motility analysis (a pause was defined as a velocity of less than  $0.085 \mu\text{m/s}$ ). Black arrow pointing to anterograde directions. (C) Average velocities and (D) corresponding histogram plot (of single event occurrences) of

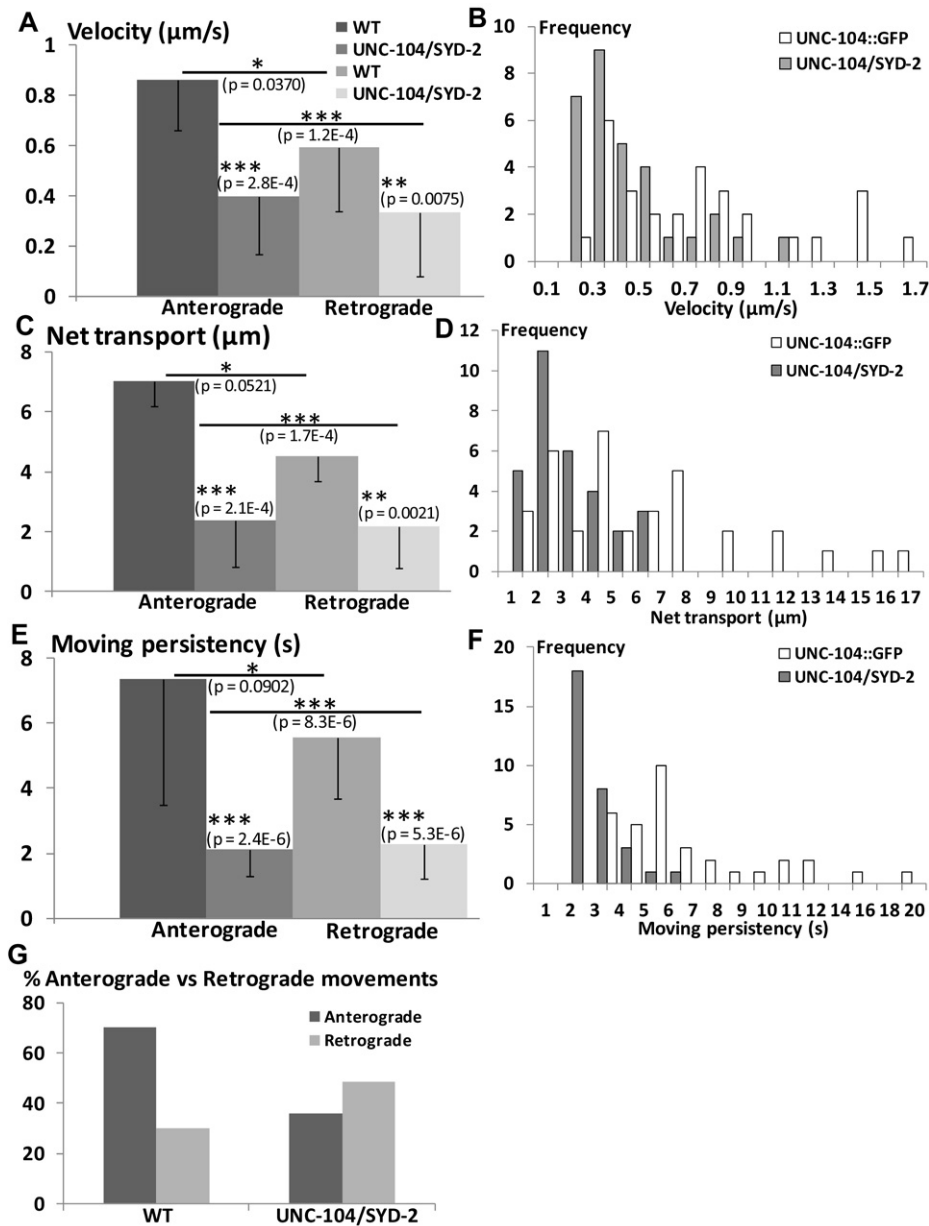


**Fig. 8.** Motility analysis of UNC-104/SYD-2 movements compared to UNC-104 alone. (A) Average velocity of UNC-104 alone (WT) and UNC-104/SYD-2 BiFC complexes (in anterograde and retrograde directions) and corresponding histogram (B). (C) Average net transport with corresponding histogram (D) and average moving persistency (E) with corresponding histogram (F). (G) Percentages of anterograde movements versus retrograde movements of UNC-104::GFP alone or UNC-104/SYD-2 BiFC complexes. WT data taken from Fig. 7. Experiments were carried out on isolated *C. elegans* neurons. \*  $P < 0.1$ , \*\*  $P < 0.05$ , \*\*\*  $P < 0.01$  Student's *t*-test. Error bars=STD.

when opposing motors are attached to the same cargo and pulling in different directions at the same time; fifth, phosphorylation of motors could act as a regulatory signal (Hirokawa and Noda, 2008; Hirokawa et al., 2009b; Schlager and Hoogenraad, 2009; Verhey and Hammond,

2009; Holzbaun and Goldman, 2010). In this study, we focus on how the cargo itself might regulate a motor's neuronal distribution.

As there are many known cargos (including a diverse amount of synaptic precursors, cytoskeletal subunits, RNA

UNC-104::GFP (wt) and UNC-104/DNC-1 BiFC pairs. (E–J) Averages and corresponding histograms of pausing duration (E, F), net transport (processivity or total run length) (G, H) and moving persistency (at uniform velocity) (I, J). Note that due to the very few movements of UNC-104/DNC-1 complexes in retrograde directions (A) we only provide data for anterograde movements in panels (C), (E), (G), and (I). Experiments were carried out on isolated *C. elegans* neurons. \*  $P < 0.1$ , \*\*  $P < 0.05$ , \*\*\*  $P < 0.01$  Student's *t*-test. Error bars=STD. For interpretation of the references to color in this figure legend, the reader is referred to the Web version of this article.

granules, mitochondria etc.) and cargo-binding to molecular motors is thought to be highly specific, we attempt to make use of an interactome map generated by [Zhong and Sternberg \(2006\)](#) to identify novel and specific cargos for the major synaptic vesicle transporter kinesin-3 UNC-104/KIF1A. Since we wish to understand how UNC-104 is allocated in different sub-cellular locations upon binding to the identified adaptors (UNC-16, DNC-1 and SYD-2) we choose to employ the BiFC assay that seemed to be an ideal method to approach our questions. For example, in FLIM-FRET assays fluorescence lifetime of the donor fluorophore can be reduced at much larger distances to an approaching acceptor fluorophore whereas in BiFC assays Venus hybrids need to directly and physically meet (interact) for successful complementation (therefore also assayed proteins need to come closer to each other). Interestingly, it has been reported that in BiFC assays even transient and weak protein interactions can be detected ([Hiatt et al., 2008](#); [Morell et al., 2008](#); [Shyu et al., 2008](#)). Still, it shall be assumed that fluorophore complementation might restrict the two (assayed) proteins from unbinding ([Hiatt et al., 2008](#)). This might explain the observed effect that UNC-104 bound to SYD-2 leads to an accumulation in distal parts of axons in the first place ([Fig. 6G–K](#)) (consistent with previous findings that SYD-2 activates and clusters UNC-104; [Wagner et al., 2009](#)); however, at a later stage, SYD-2's disability to unbind from the motor would lead to the observed reduction in UNC-104's motility qualities ([Fig. 8](#)). The motor's restriction to move freely was also evident in time-lapse images as we mostly recorded short moving distances between two consecutive axonal motor-clusters. This finding can be explained by increased SYD-2/SYD-2 self-interactions (SYD-2's ability to oligomerize has been reported; [Kim et al., 2001](#); [Wagner et al., 2009](#)), and if assumed that SYD-2 cannot unbind from the motor, the motor itself would cluster and therefore being restricted from moving properly.

### The effects of dynactin p150<sup>Glued</sup> interaction with UNC-104

As mentioned above, frequent observed bidirectional movements of synaptic vesicles can be explained by binding of opposing motors to the same vesicle and pulling in antagonistic directions. If opposing motors (as kinesin and dynein motors) are activated at the same time and physically attached to a microtubule they might be involved (at least for short runs) in a tug-of-war situation. For longer runs, it is assumed that coordinated motor activity controls the directionality of a vesicular cargo ([Welte, 2004](#); [Hendricks et al., 2010](#); [Holzbaur and Goldman, 2010](#)). Indeed, direct and functional interactions between dynactin and kinesin-2 ([Deacon et al., 2003](#); [Berezuk and Schroer, 2007](#)) as well as between dynein and kinesin-1 ([Ligon et al., 2004](#)) have been reported. Further, in both *C. elegans* and *Drosophila*, UNC-104-mediated transport of synaptic vesicles requires dynein ([Koushika et al., 2004](#); [Barkus et al., 2008](#)). Still, a direct and functional interaction between the kinesin-3 UNC-104 and dynactin remains to be investigated. Here we show that the dynactin subunit p150<sup>Glued</sup>

(DNC-1) modulates UNC-104's allocation in neurons ([Fig. 5](#)) and also affects the motor's motility characteristics ([Fig. 7](#)). The biased localization of UNC-104 to axonal endings when bound to DNC-1 (compare [Figs. 1 and 5](#)) might be explained by an exclusion of other important dynactin subunits (dynamitin, Arp1 etc.) by the Venus fluorophore. Which means even the long linker between the Venus and the UNC-104/DNC-1 complex might not prevent sterical exclusion of a further binding partner. Therefore dynactin assembly could be incomplete and retrograde transport of the UNC-104/DNC-1 complex by dynein restricted. Note that we decided to fuse the Venus hybrid to the C-terminus of DNC-1 (that associates with dynamitin) as the N-terminus contains the important Cap-Gly domain that interacts with microtubules while central domains of DNC-1 contain the dynein-binding site.

### Consequences of UNC-104 distribution upon binding to UNC-16

[Byrd et al. \(2001\)](#) describe a model in which UNC-16 (a homolog of mouse JSAP1/JIP3 and *Drosophila* Sunday Driver) regulates kinesin-1 mediated vesicle transport in *C. elegans*. Since *unc-16* mutations partially suppress the vesicle retention defect in *unc-104* mutants, they also proposed that UNC-16 might facilitate the exchange between UNC-104 and kinesin-1 (UNC-116) on a vesicular cargo. In addition, the group suggests that a complex of UNC-16 and UNC-116 (linked via kinesin-light chain KLC-2) might restrain UNC-104-bound vesicles from moving to dendrites and in turn would facilitate UNC-104-driven vesicle transport towards axons. Interestingly, it has been shown that JIP3 also associates with dynactin (through the p150<sup>Glued</sup> domain) and that ADP-ribosylation factor 6 (ARF6, a small G protein regulating endosome trafficking) controls JIP3's switching from kinesin-1 to dynactin ([Montagnac et al., 2009](#)). In our present study we have shown (for the first time) a direct interaction between UNC-16 and UNC-104 and the resulting consequences for the motor's allocation. From [Fig. 3](#) it is evident that UNC-104 bound to UNC-16 retains in soma to a large extent suggesting a novel regulatory role for UNC-16 on a kinesin-3 motor. As we have no evidence whether or not UNC-16 is bound to KLC-2 while associating with UNC-104 we can neither confirm nor negate the proposed model by [Byrd et al. \(2001\)](#). Also, since [Byrd et al. \(2001\)](#) investigated synaptic vesicles markers, while we focus on the motor itself, our experimental approaches are different. Still, it is obvious that UNC-16 plays a role in regulating both neuronal motors, kinesin-1 UNC-116 and kinesin-3 UNC-104 and future studies are encouraged to understand the molecular basis of UNC-16-mediated regulation of these important axonal motors.

## CONCLUSION

To understand the basis of bidirectional movement of synaptic vesicles, models have been developed in which motors of opposing directionality are attached to the same vesicle and their activity is coordinated by factors (as adaptor proteins). Dynactin has been proposed to be a key

regulator for controlling alternating activity of kinesin and dynein motors. Here, we demonstrate for the first time a direct binding between dynactin and the major synaptic vesicle transporter UNC-104(KIF1A) and the resulting consequences for the motor's motility and neuronal distribution. Similarly, we demonstrate a direct role of UNC-16, suggested to be a crucial factor for kinesin-1/kinesin-3 regulation, on UNC-104's allocation. Together, we provide evidence that the adaptor proteins UNC-16, SYD-2 and DNC-1 engage in critical but distinct roles on UNC-104 regulation.

*Acknowledgments*—We like to thank Dr. Chang-Deng Hu's Lab (Purdue University, USA) for providing the BiFC positive control vector kit. Thanks to National Synchrotron Radiation Research Center (Hsinchu, Taiwan) for the use of an Olympus FV1000 and for providing us an Andor iXon DV887 EMCCD camera. Nematode strains were provided by the *Caenorhabditis Genetics Center* (CGC), which is funded by the National Institutes of Health National Center for Research Resources. This work was supported by the National Science Council of Taiwan Grant 97-2311-B-007-006-MY3 to O.I.W.

## REFERENCES

- Barkus RV, Klyachko O, Horiuchi D, Dickson BJ, Saxton WM (2008) Identification of an axonal kinesin-3 motor for fast anterograde vesicle transport that facilitates retrograde transport of neuropeptides. *Mol Biol Cell* 19:274–283.
- Berezuk MA, Schroer TA (2007) Dynactin enhances the processivity of kinesin-2. *Traffic* 8:124–129.
- Brenner S (1974) The genetics of *Caenorhabditis elegans*. *Genetics* 77:71–94.
- Brown HM, Van Epps HA, Goncharov A, Grant BD, Jin Y (2009) The JIP3 scaffold protein UNC-16 regulates RAB-5 dependent membrane trafficking at *C. elegans* synapses. *Dev Neurobiol* 69:174–190.
- Byrd DT, Kawasaki M, Walcoff M, Hisamoto N, Matsumoto K, Jin Y (2001) UNC-16, a JNK-signaling scaffold protein, regulates vesicle transport in *C. elegans*. *Neuron* 32:787–800.
- Chevalier-Larsen E, Holzbaur EL (2006) Axonal transport and neurodegenerative disease. *Biochim Biophys Acta* 1762:1094–1108.
- Christensen M, Estevez A, Yin X, Fox R, Morrison R, McDonnell M, Gleason C, Miller DM 3rd, Strange K (2002) A primary culture system for functional analysis of *C. elegans* neurons and muscle cells. *Neuron* 33:503–514.
- Deacon SW, Serpinskaya AS, Vaughan PS, Lopez Fanarraga M, Vernos I, Vaughan KT, Gelfand VI (2003) Dynactin is required for bidirectional organelle transport. *J Cell Biol* 160:297–301.
- De Vos KJ, Grierson AJ, Ackerley S, Miller CC (2008) Role of axonal transport in neurodegenerative diseases. *Annu Rev Neurosci* 31:151–173.
- Duncan JE, Goldstein LS (2006) The genetics of axonal transport and axonal transport disorders. *PLoS Genet* 2:e124.
- Hall DH, Hedgecock EM (1991) Kinesin-related gene unc-104 is required for axonal transport of synaptic vesicles in *C. elegans*. *Cell* 65:837–847.
- Hendricks AG, Perlson E, Ross JL, Schroeder HW 3rd, Tokito M, Holzbaur EL (2010) Motor coordination via a tug-of-war mechanism drives bidirectional vesicle transport. *Curr Biol* in press.
- Hiatt SM, Shyu YJ, Duren HM, Hu CD (2008) Bimolecular fluorescence complementation (BiFC) analysis of protein interactions in *Caenorhabditis elegans*. *Methods* 45:185–191.
- Hirokawa N, Nitta R, Okada Y (2009a) The mechanisms of kinesin motor motility: lessons from the monomeric motor KIF1A. *Nat Rev Mol Cell Biol* 10:877–884.
- Hirokawa N, Noda Y (2008) Intracellular transport and kinesin superfamily proteins, KIFs: structure, function, and dynamics. *Physiol Rev* 88:1089–1118.
- Hirokawa N, Noda Y, Tanaka Y, Niwa S (2009b) Kinesin superfamily motor proteins and intracellular transport. *Nat Rev Mol Cell Biol* 10:682–696.
- Holzbaur EL, Goldman YE (2010) Coordination of molecular motors: from *in vitro* assays to intracellular dynamics. *Curr Opin Cell Biol* 22:4–13.
- Hu CD, Chinenov Y, Kerppola TK (2002) Visualization of interactions among bZIP and Rel family proteins in living cells using bimolecular fluorescence complementation. *Mol Cell* 9:789–798.
- Hu CD, Kerppola TK (2003) Simultaneous visualization of multiple protein interactions in living cells using multicolor fluorescence complementation analysis. *Nat Biotechnol* 21:539–545.
- Inomata H, Nakamura Y, Hayakawa A, Takata H, Suzuki T, Miyazawa K, Kitamura N (2003) A scaffold protein JIP-1b enhances amyloid precursor protein phosphorylation by JNK and its association with kinesin light chain 1. *J Biol Chem* 278:22946–22955.
- Kaether C, Skehel P, Dotti CG (2000) Axonal membrane proteins are transported in distinct carriers: a two-color video microscopy study in cultured hippocampal neurons. *Mol Biol Cell* 11:1213–1224.
- Kamal A, Stokin GB, Yang Z, Xia CH, Goldstein LS (2000) Axonal transport of amyloid precursor protein is mediated by direct binding to the kinesin light chain subunit of kinesin-I. *Neuron* 28:449–459.
- Kelkar N, Delmotte MH, Weston CR, Barrett T, Sheppard BJ, Flavell RA, Davis RJ (2003) Morphogenesis of the telencephalic commissure requires scaffold protein JNK-interacting protein 3 (JIP3). *Proc Natl Acad Sci U S A* 100:9843–9848.
- Kerppola TK (2006a) Design and implementation of bimolecular fluorescence complementation (BiFC) assays for the visualization of protein interactions in living cells. *Nat Protoc* 1:1278–1286.
- Kerppola TK (2006b) Visualization of molecular interactions by fluorescence complementation. *Nat Rev Mol Cell Biol* 7:449–456.
- Kim CA, Phillips ML, Kim W, Gingery M, Tran HH, Robinson MA, Faham S, Bowie JU (2001) Polymerization of the SAM domain of TEL in leukemogenesis and transcriptional repression. *EMBO J* 20:4173–4182.
- Kocsis E, Trus BL, Steer CJ, Bisher ME, Steven AC (1991) Image averaging of flexible fibrous macromolecules: the clathrin triskelion has an elastic proximal segment. *J Struct Biol* 107:6–14.
- Koushika SP (2008) “JIP”ing along the axon: the complex roles of JIPs in axonal transport. *Bioessays* 30:10–14.
- Koushika SP, Schaefer AM, Vincent R, Willis JH, Bowerman B, Nonet ML (2004) Mutations in *Caenorhabditis elegans* cytoplasmic dynein components reveal specificity of neuronal retrograde cargo. *J Neurosci* 24:3907–3916.
- Ligon LA, Tokito M, Finklestein JM, Grossman FE, Holzbaur EL (2004) A direct interaction between cytoplasmic dynein and kinesin I may coordinate motor activity. *J Biol Chem* 279:19201–19208.
- Matsuda S, Matsuda Y, D'Adamio L (2003) Amyloid beta protein precursor (AbetaPP), but not AbetaPP-like protein 2, is bridged to the kinesin light chain by the scaffold protein JNK-interacting protein 1. *J Biol Chem* 278:38601–38606.
- Mello CC, Kramer JM, Stinchcomb D, Ambros V (1991) Efficient gene transfer in *C. elegans*: extrachromosomal maintenance and integration of transforming sequences. *EMBO J* 10:3959–3970.
- Montagnac G, Sibarita JB, Loubery S, Daviet L, Romao M, Raposo G, Chavrier P (2009) ARF6 interacts with JIP4 to control a motor switch mechanism regulating endosome traffic in cytokinesis. *Curr Biol* 19:184–195.
- Morell M, Espargaro A, Aviles FX, Ventura S (2008) Study and selection of *in vivo* protein interactions by coupling bimolecular fluorescence complementation and flow cytometry. *Nat Protoc* 3:22–33.
- Morfini GA, Burns M, Binder LI, Kanaan NM, LaPointe N, Bosco DA, Brown RH Jr., Brown H, Tiwari A, Hayward L, Edgar J, Nave KA,

- Garberm J, Atagi Y, Song Y, Pigino G, Brady ST (2009) Axonal transport defects in neurodegenerative diseases. *J Neurosci* 29:12776–12786.
- Olsen O, Moore KA, Nicoll RA, Bredt DS (2006) Synaptic transmission regulated by a presynaptic MALS/Liprin-alpha protein complex. *Curr Opin Cell Biol* 18:223–227.
- Sakamoto R, Byrd DT, Brown HM, Hisamoto N, Matsumoto K, Jin Y (2005) The *Caenorhabditis elegans* UNC-14 RUN domain protein binds to the kinesin-1 and UNC-16 complex and regulates synaptic vesicle localization. *Mol Biol Cell* 16:483–496.
- Schlager MA, Hoogenraad CC (2009) Basic mechanisms for recognition and transport of synaptic cargos. *Mol Brain* 2:25.
- Setou M, Seog DH, Tanaka Y, Kanai Y, Takei Y, Kawagishi M, Hirokawa N (2002) Glutamate-receptor-interacting protein GRIP1 directly steers kinesin to dendrites. *Nature* 417:83–87.
- Shyu YJ, Hiatt SM, Duren HM, Ellis RE, Kerppola TK, Hu CD (2008) Visualization of protein interactions in living *Caenorhabditis elegans* using bimolecular fluorescence complementation analysis. *Nat Protoc* 3:588–596.
- Stokin GB, Goldstein LS (2006) Axonal transport and Alzheimer's disease. *Annu Rev Biochem* 75:607–627.
- Strange K, Christensen M, Morrison R (2007) Primary culture of *Caenorhabditis elegans* developing embryo cells for electrophysiological, cell biological and molecular studies. *Nat Protoc* 2:1003–1012.
- Verhey KJ, Hammond JW (2009) Traffic control: regulation of kinesin motors. *Nat Rev Mol Cell Biol* 10:765–777.
- Verhey KJ, Meyer D, Deehan R, Blenis J, Schnapp BJ, Rapoport TA, Margolis B (2001) Cargo of kinesin identified as JIP scaffolding proteins and associated signaling molecules. *J Cell Biol* 152:959–970.
- Wagner OI, Esposito A, Kohler B, Chen CW, Shen CP, Wu GH, Butkevich E, Mandalapu S, Wenzel D, Wouters FS, Klopfenstein DR (2009) Synaptic scaffolding protein SYD-2 clusters and activates kinesin-3 UNC-104 in *C. elegans*. *Proc Natl Acad Sci U S A* 106:19605–19610.
- Welte MA (2004) Bidirectional transport along microtubules. *Curr Biol* 14:R525–R537.
- Yonekawa Y, Harada A, Okada Y, Funakoshi T, Kanai Y, Takei Y, Terada S, Noda T, Hirokawa N (1998) Defect in synaptic vesicle precursor transport and neuronal cell death in KIF1A motor protein-deficient mice. *J Cell Biol* 141:431–441.
- Zal T (2008) Visualization of protein interactions in living cells. *Adv Exp Med Biol* 640:183–197.
- Zhong W, Sternberg PW (2006) Genome-wide prediction of *C. elegans* genetic interactions. *Science* 311:1481–1484.
- Zhou HM, Brust-Mascher I, Scholey JM (2001) Direct visualization of the movement of the monomeric axonal transport motor UNC-104 along neuronal processes in living *Caenorhabditis elegans*. *J Neurosci* 21:3749–3755.

(Accepted 23 December 2010)  
(Available online 30 December 2010)